

CONTRIBUTIONS IN THE DOMAIN OF THE CONTACT STRESSES BETWEEN CYLINDERS OF COLD ROLLING

A.D. MAIMON¹, D. BOAZU², L. STOICESCU²

¹ARCELOR – Mittal Steel Galati

²"Dunărea de Jos" University of Galați
email: dboazu@ugal.ro

ABSTRACT

Elasto-plastic contact stresses between working cylinder and support cylinder of cold rolling using FEM are presented in this paper. Pressure and tractions resulted from the rolling process were obtained by using a calculus program and they were used as loads on a working cylinder.

KEYWORDS: cold rolling, elasto-plastic contact stresses, rolling process

1. FEM model of contact between working cylinder (585mm) and support cylinder(1525mm) of cold rolling

For the modelling process COSMOS/M version 2.5 was used. The two cylinders were modelled using PLANE2D (plane strain) elements with 4 nodes and two degrees of freedom per node. 2D model is represented in Fig. 1. A zoom of fin mesh in the vicinity of contact between the two cylinders is presented in Fig. 3 and the mesh in loading zone (load is given by normal and tangential pressure from

rolling process) is represented in Fig. 2. The whole model has 14517 nodes and 17101 elements.

One node GAP elements (in 2D node-line contact elements) were used for transmission of stresses and deformations through contact zone.

The two cylinders were considered supported by elastic elements whose rigidity is given by that of the rolling system. Working with GAP elements imposed an incremental loading and so the analysis is static but nonlinear.

The contact between cylinders is a non-conforming contact problem because the extension of contact zone is not known from the beginning.

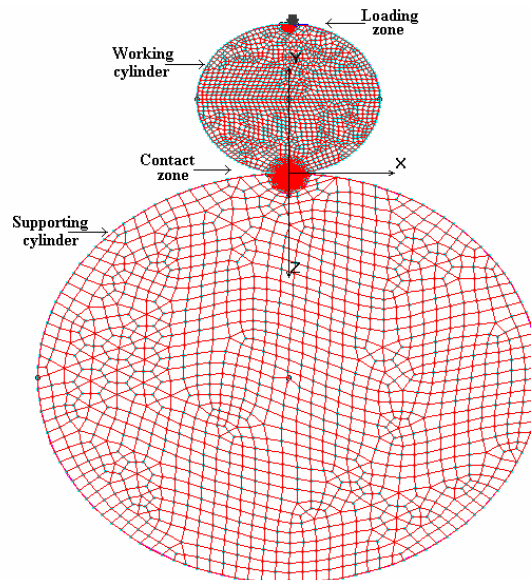


Fig. 1. FEM model between working cylinder and support cylinder of cold rolling.

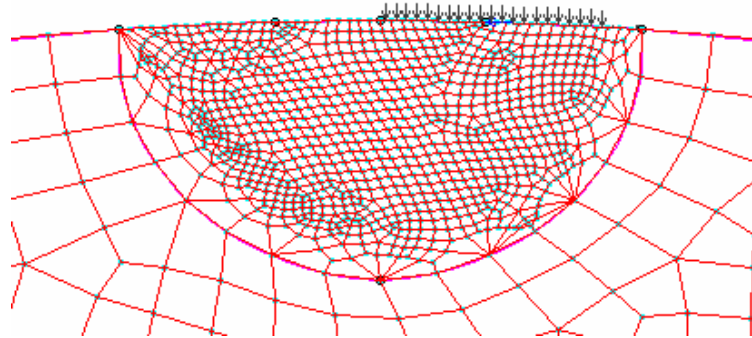


Fig. 2. Mesh in loading zone of working cylinder

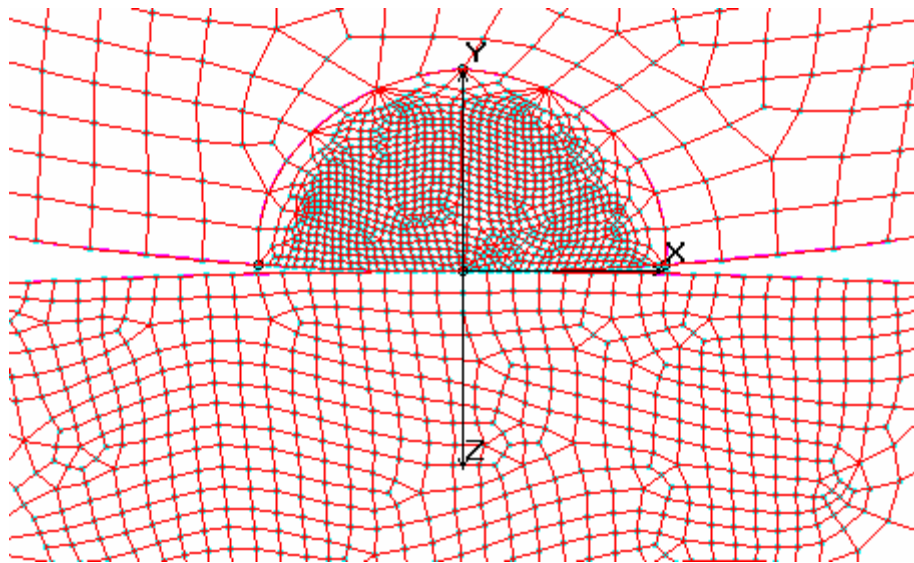


Fig. 3. Mesh in contact zone between the two cylinders

2. Material model

The elasto plastic behaviour of material (special steel) of the two cylinders was considered von Mises with isotropic hardening. Principal parameters of material model are: Young modulus $E=2.1 \cdot 10^4$ daN/mm², Poisson ratio 0.3, yield stress 73 daN/mm², and tangent modulus 20daN/mm².

3. Studied cases

It was analyzed two cases with the 5 phases of sheet thickness reduction. (17.7%, 20.6%, 24.2%, 20.8, 17.5%). In the first case the friction coefficient was considered $\mu=0.1$ and in the second case friction coefficient was considered $\mu=0.075$. The width of the sheet was considered 1250mm.

The loading conditions for cold rolling were established according to reference [3].

For these analyzed cases the equivalent von Mises stress distribution and principal stresses are represented in Fig. 4-8 ($\mu=0.1$) and Fig. 9-13

($\mu=0.075$). The extension of contact zone is of 40mm. The contact stain extends to about 40 mm.

The results of nonlinear analysis are given in Table 1 (Case 1 ($\mu=0.1$)) and Table 2 (Case 1 ($\mu=0.1$))-von Mises stresses from contact zone (σ_{ech}^* - for working cylinder) and (σ_{ech}^{**} - for supporting cylinder) and principal stresses in the contact zone $\sigma_1, \sigma_2, \sigma_3$. The stress state in the vicinity of contact is 3D. In Tables 1 and 2 principal stresses $\sigma_1 < \sigma_2 < \sigma_3$ are negative values and the biggest one σ_3 is considered the contact stress (Hertzian pressure). The equivalent von Mises stress was evaluated at a distance of 2 mm from contact effective zone, because in the contact zone the components of deviator tensor are unmeaningful.

The influence of friction on loading and contact behaviour was considered by modifying friction coefficient ($\mu=0.1$ for dry friction) and ($\mu=0.075$ for lubrication).

The equivalent von Mises stress is calculated using the formula:

$$VON = \left\{ \frac{1}{2} [(\sigma_X - \sigma_Y)^2 + (\sigma_X - \sigma_Z)^2 + (\sigma_Y - \sigma_Z)^2] + 3(\tau_{XY}^2 + \tau_{XZ}^2 + \tau_{YZ}^2) \right\}^{(1/2)}$$

$$VON = \left\{ \frac{1}{2} [(\sigma_1 - \sigma_2)^2 + (\sigma_1 - \sigma_3)^2 + (\sigma_2 - \sigma_3)^2] \right\}^{(1/2)}$$

Or by means of principal stresses:

Table 1

Case 1 ($\mu=0.1$)	σ_{ech}^* [daN/mm ²]	σ_{ech}^{**} [daN/mm ²]	$\sigma_{1,max}$ [daN/mm ²]	$\sigma_{2,max}$ [daN/mm ²]	$\sigma_{3,max}$ [daN/mm ²]
Phase A1	72.95	72.95	79.95	117.97	150.91
Phase A2	73	73	150.4	178.9	215.5
Phase A3	73	73	156.068	184.79	230.258
Phase A4	72.99	72.99	130.989	146.134	200.24
Phase A5	73.563	73.563	253.754	289.142	330.84

Table 2

Case 1 ($\mu=0.075$)	σ_{ech}^* [daN/mm ²]	σ_{ech}^{**} [daN/mm ²]	$\sigma_{1,max}$ [daN/mm ²]	$\sigma_{2,max}$ [daN/mm ²]	$\sigma_{3,max}$ [daN/mm ²]
Phase F A1	72.953	72.953	73.389	108.123	136.507
Phase F A2	72.890	72.890	81.960	118.186	153.887
Phase F A3	73.044	73.044	141.576	172.475	217.362
Phase F A4	72.937	72.937	105.476	129.328	169.797
Phase F A5	73.036	73.036	167.813	197.075	241.869

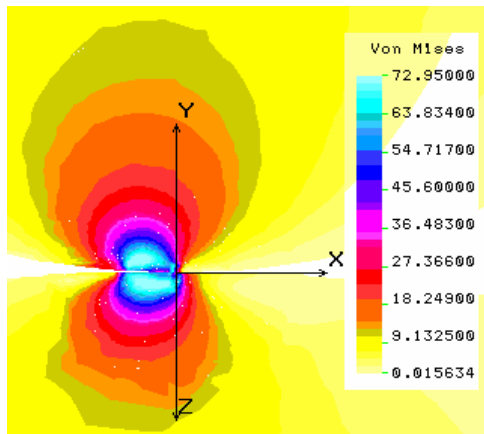


Fig. 4a. Case 1 ($\mu=0.1$) Phase A1
von Mises stress

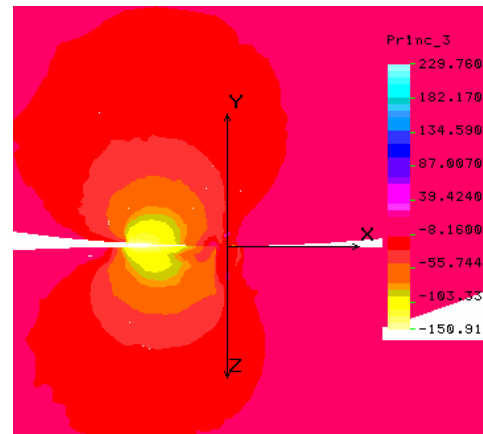


Fig.4b. Case 1 ($\mu=0.1$) Phase A1
principal stress σ_3

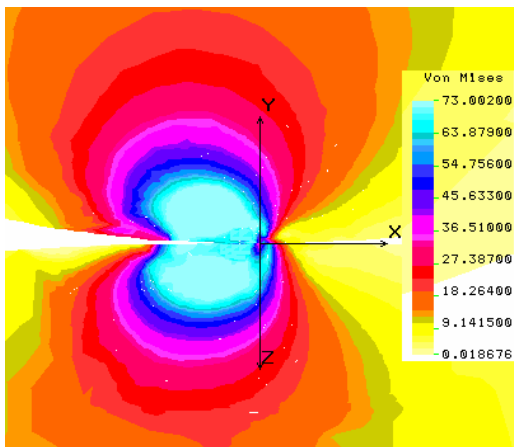


Fig. 5a. Case 1 ($\mu=0.1$) Phase A2
von Mises stress

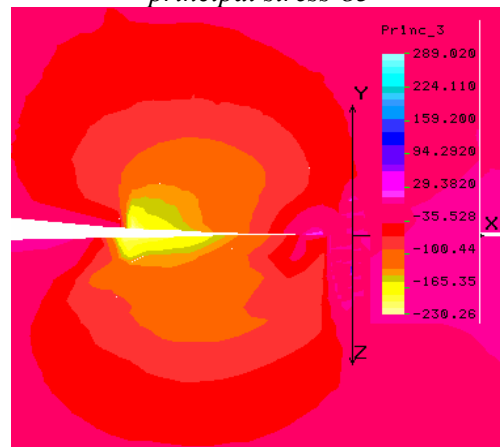


Fig. 5b. Case 1 ($\mu=0.1$) Phase A2
principal stress σ_3

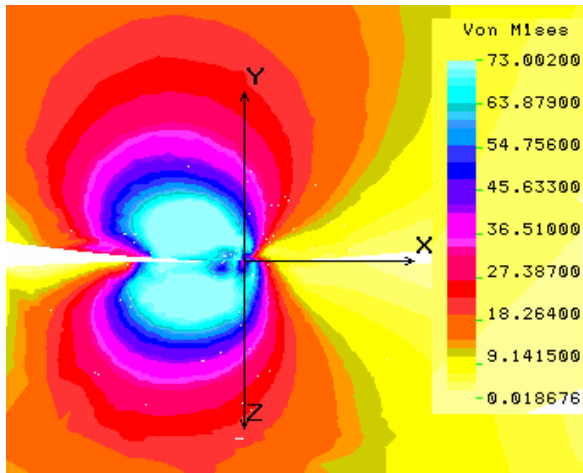


Fig. 6a. Case 1 ($\mu=0.1$) Phase A3
 von Mises stress

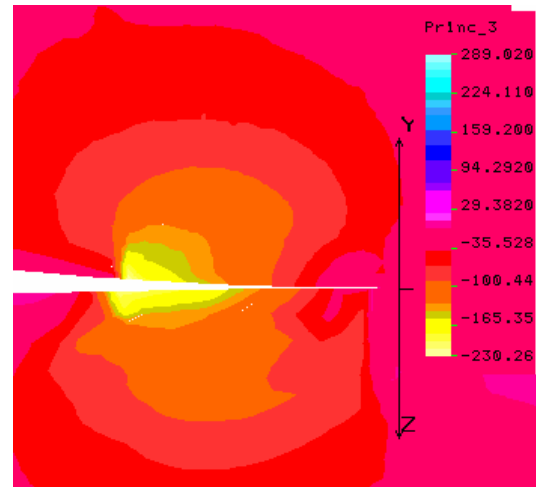


Fig. 6b. Case 1 ($\mu=0.1$) Phase A3
 principal stress σ_3

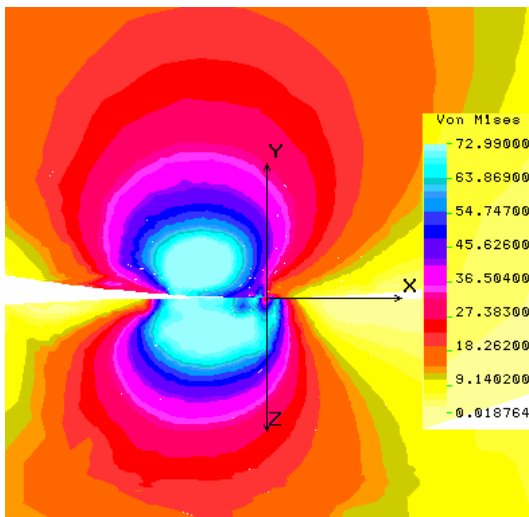


Fig. 7a. Case 1 ($\mu=0.1$) Phase A4
 principal stress σ_3

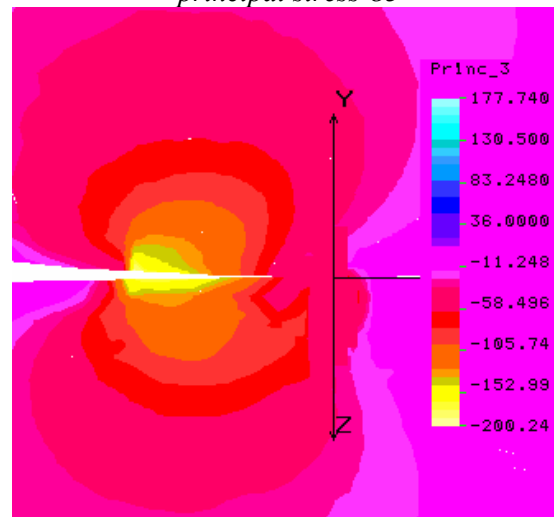


Fig. 7b. Case 1 ($\mu=0.1$) Phase A4
 principal stress σ_3

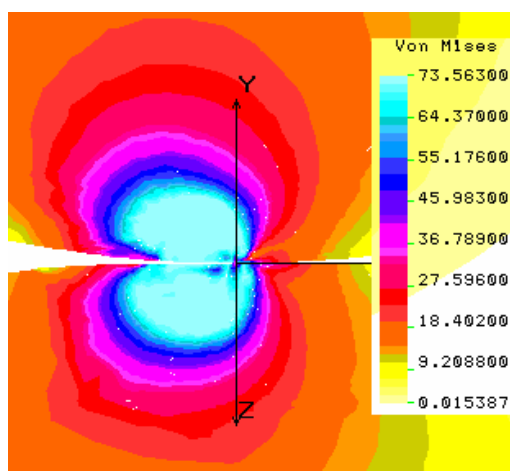


Fig. 8a. Case 1 ($\mu=0.1$) Phase A5
 principal stress σ_3

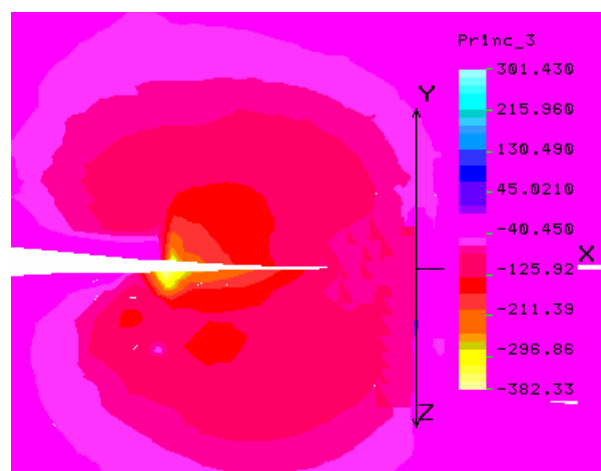


Fig. 8b. Case 1 ($\mu=0.1$) Phase A5
 principal stress σ_3

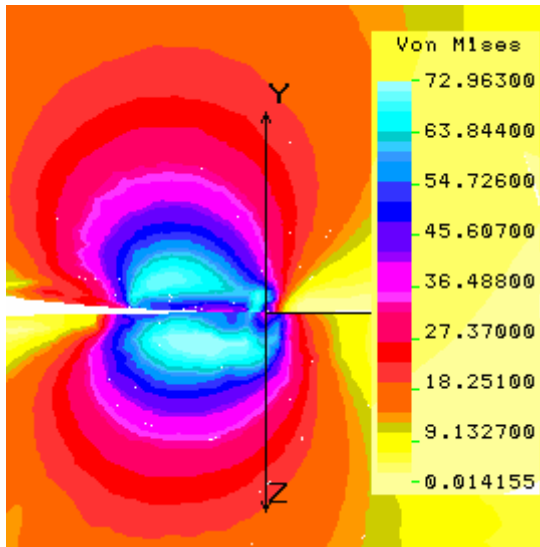


Fig. 9a. Case 2 ($\mu=0.075$) Phase F_A1 principal stress σ_3

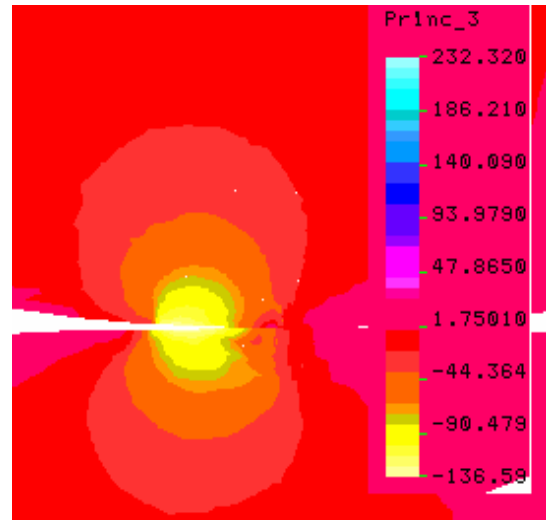


Fig. 9b. Case 2 ($\mu=0.075$) Phase F_A1 principal stress σ_3

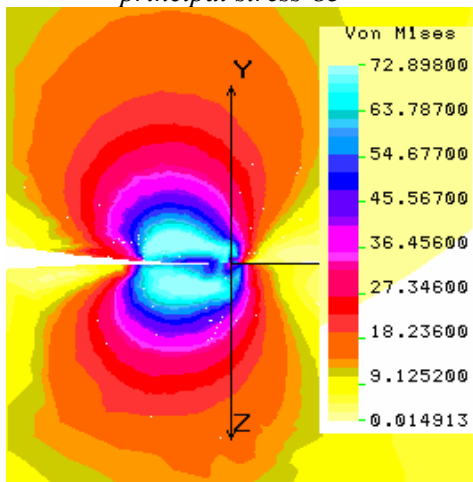


Fig. 10a. Case 2 ($\mu=0.075$) Phase F_A2 principal stress σ_3

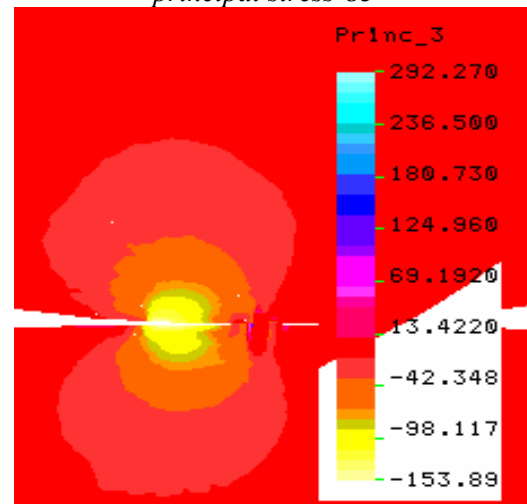


Fig. 10b. Case 2 ($\mu=0.075$) Phase F_A2 principal stress σ_3

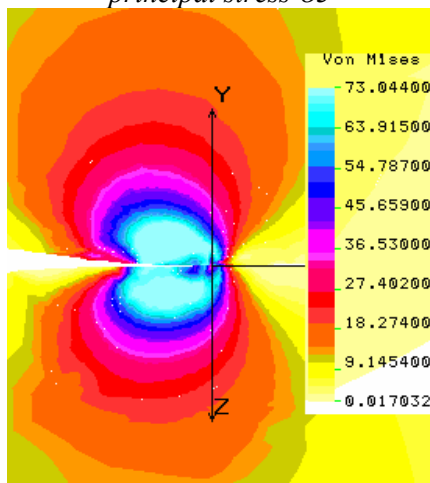


Fig. 11a. Case 2 ($\mu=0.075$) Phase F_A3 principal stress σ_3

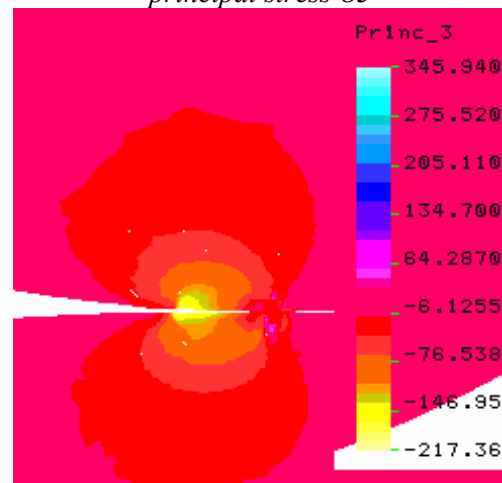


Fig. 11b. Case 2 ($\mu=0.075$) Phase F_A3 principal stress σ_3

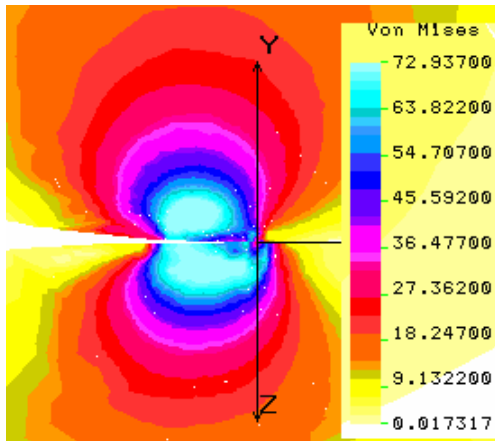


Fig. 12a. Case 2 ($\mu=0.075$) Phase F_A4 principal stress σ_3

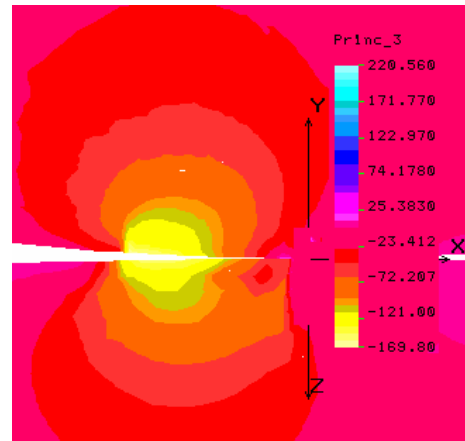


Fig. 12b. Case 2 ($\mu=0.075$) Phase F_A4 principal stress σ_3

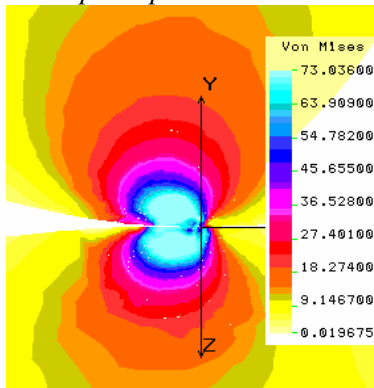


Fig. 13a. Case 2 ($\mu=0.075$) Phase F_A4 principal stress σ_3

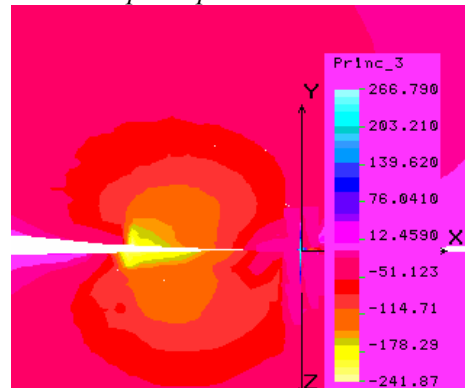


Fig. 13b. Case 2 ($\mu=0.075$) Phase F_A4 principal stress σ_3

4. Conclusions

From Fig. 14 one can observe that contact stresses are bigger when the rolling process is not lubricated.

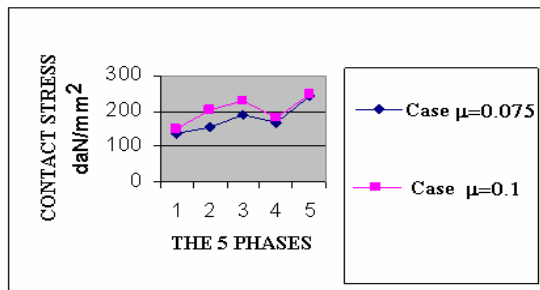


Fig. 14.

For all loading cases there are important plastic zones of elliptic shape. In the worst loading case (Case 1 ($\mu=0.1$) Phase A5 - see table 1) this elliptic region is determined by the two semiaxes of 30mm and 25mm; the eccentricity of this plastic zone in respect to vertical axis of the two cylinders is about 40mm.

References

- [1]. Bern A., 1990, *Le laminage a froid*, Symposium franco-roumain, Galati.
- [2]. Poloukhine V., 1977, *Simulation mathematique et calcul sur ordinateur des laminoirs a toles*, Edition MIR, Moscou.
- [3]. Stoicescu L., Gavrilescu I., Boazu D., 1995, *Algoritm și program pentru modelarea laminării la rece*, Asociația oamenilor de știință, filiala Galați, Departamentul de Inginerie Tehnologică și Deformare Plastică, tom 21, octombrie 1995, pg. 123-128.